EURASIAN PHYSICAL TECHNICAL JOURNAL

2025, Volume 22, No. 2 (52)

https://doi.org/10.31489/2025N2/33-41

Received: 26/02/2025 Revised: 16/04/2025 Accepted: 23/06/2025 Published online: 30/06/2025
Research Article

UDC 539.171

A COMPREHENSIVE PHENOMENOLOGICAL, SEMI-MICROSCOPIC, AND CRC ANALYSIS OF ^{15}N ELASTIC SCATTERING FROM ^{13}C AND ^{19}F NUCLEI

Akhat R.[1,3], Amangeldi N.[1,2], Baratova A. A.*[1], Anuar A.[1], Raiymbekov Ye. [1,3], Yergaliuly G. [1,3]

[1] L. N. Gumilyov Eurasian National University, Astana, Kazakhstan
[2] Institute of Nuclear Physics, Almaty, Kazakhstan
[3] National Laboratory Astana, Nazarbayev University, Astana
*Corresponding author: baratova_aa@enu.kz

Abstract. *In the present study, the angular distributions obtained at beam energies E_{lab} = 30.0, 32.0 and 45.0 MeV for the $^{15}N+^{13}C$ reaction and E_{lab} = 23.0, 26.0 and 29.0 MeV for the $^{15}N+^{19}F$ system were subjected to a comprehensive reanalysis using the optical model, the double folding model, and the coupled reaction channel (CRC) method. The main objective of the study was to establish the optimal optical potential through phenomenological and semi-microscopic analysis. Through careful calculations, the acceptable parameters of the potentials and their energy dependencies were derived for both nuclear systems. Notably, the angular distributions were well reproduced, indicating the effectiveness of the theoretical models used. In back angle scattering analysis, the CRC has very good agreement with the experimental values. As a result of the analysis, spectroscopic amplitudes were extracted for the $^{15}N \rightarrow {}^{13}C + d$ and $^{19}F \rightarrow {}^{15}N + \alpha$ configurations at different energies of the incident ^{15}N ions. The obtained results of spectroscopic amplitudes were subsequently compared with previously reported values, facilitating an assessment of the consistency and accuracy of the present work.*

Keywords: elastic scattering, optical model, double-folding model, elastic transfer, spectroscopic amplitude.

1. Introduction

Elastic scattering in nuclear physics is a key method for studying nuclear structure and nucleon-nucleon interactions. The angular distribution of scattered particles, resembling light diffraction by an opaque disk, is effectively analyzed using the optical model (OM), which provides a reliable framework for describing scattering phenomena [1]. Elastic scattering data helps map nuclear matter distribution and understand nuclear properties. Among various theoretical models, including the shell and cluster models, the OM has been a cornerstone in analyzing charged particle scattering for decades. The OM is commonly used to describe the scattering of different systems, including elastic [2–7] and elastic transfer [8–11] scattering.

In this study, OM is applied to analyze the angular distribution of elastic scattering for the $^{15}N+^{13}C$ and $^{15}N+^{19}F$ nuclear systems. The goal is to identify the optimal optical potential, refine its parameters, and determine reaction cross sections. Early investigations in this field began with Gamp A. [12] in 1975, who studied $^{15}N+^{13}C$ scattering at energies of 30.0, 32.0, and 45.0 MeV, using phenomenological Woods-Saxon potentials. Later, Gamp A. in [13] extended work to $^{15}N+^{19}F$ scattering at energies of 23.0, 26.0, and 29.0 MeV, analyzing differential cross sections with a range of complex potentials. By incorporating OM into the analysis, this study provides deeper insights into the nuclear interactions of these systems. In practice,

multiple parameters set often provide equally good fits to the data, raising the critical question of whether some are more physically meaningful than others, and, if so, which should be prioritized. This emphasizes the need to assess the physical relevance of each parameter set and choose the most suitable one to ensure the results are both reliable and easy to interpret.

Accurately determining the optical potential through phenomenological analysis alone is challenging due to ambiguities in the complex parameter space. Thus, it is essential to constrain the potential within physical boundaries before parameter optimization. To address this, the double-folding model (DF) is employed to identify physically meaningful optical potential parameters [14–17].

In this study, we investigate the ^{15}N+ ^{13}C and ^{15}N+ ^{19}F nuclear systems using the standard optical model, combining both phenomenological and semi-microscopic approaches. Experimental angular distribution data were analyzed with the FRESCO and SFRESCO codes [18] to derive nuclear potentials and reaction cross-section parameters. The organization of the manuscript is as follows: section 1 Introduction, section 2 research within the framework of OM and DF with suitable optical parameters of the potentials. Section 3 analyzes the data within the CRC, presenting the results and leading the discussion. The conclusion is presented in section 4.

2. OM, DF analysis of ^{15}N +^{13}C, ^{15}N+ ^{19}F

The experimental data for the ^{15}N+ ^{13}C and ^{15}N+ ^{19}F nuclear systems were reanalyzed phenomenologically and semi-microscopically under the standard OM. In the first approach, the differential cross-sections were calculated in the framework of the phenomenological OM, and the interaction potential was found by fitting the computed cross-sections to the experimental data.

Within this model, the total interaction potential has a shape:

$$U(r) = -V_0\left[1+\exp\left(\frac{r-R_V}{a_V}\right)\right]^{-1} - iW_0\left[1+\exp\left(\frac{r-R_W}{a_W}\right)\right]^{-1} + V_c(r), \quad (1)$$

where V_0 real potential depth, W_0 imaginary potential depth, a_W, a_V are the diffuseness of real and imaginary potential parts; r_V, r_W: the reduced radii of these potential parts. These six parameters were allowed to vary independently.

$V_c(r)$ the Coulomb potential is defined as follows [19]:

$$V_C(r) = \begin{cases} \dfrac{Z_1 Z_2 e^2}{2R_C}\left(3-\dfrac{r^2}{R_C}\right) & \text{for r}<R_C \\ \dfrac{Z_1 Z_2 e^2}{r} & \text{for r} \geq R_C \end{cases}, \quad (2)$$

where R_C -Coulomb potential radius.

The optical potential can also be determined using semi-microscopic methods [20], which incorporate the internal structure of the interacting nuclei. In this approach, the nuclear-nuclear potential is derived from the nucleon-nucleon (NN) interaction [21, 22]. Effective NN interaction takes into account even and odd components of the central forces. The real potential is the sum of direct and exchange potentials[23]:

$$\vec{V} = V^D + V^{EX}. \quad (3)$$

The direct term of folding potential is given by:

$$V^D(R) = \iint \rho^{(1)}(r_1) v_D(s) \rho^{(2)}(r_2) dr_1 dr_2, \quad (4)$$

where, $v^D(s)$ - is the direct component of the effective NN interaction, $\rho^{(1)}$, $\rho^{(2)}$ - densities of colliding nuclei, R -distance between nucleus $\left|\vec{R}\right|$.

Exchange term of folding potential is given by the expression:

$$V^{EX}(R) = \iint \rho^{(1)}(r_1, r_1+s) v_{EX}(s) \rho^{(2)}(r_2, r_2+s) \exp\left[ik(R)s/M\right] dr_1 dr_2, \quad (5)$$

where $v_{EX}(s)$ - is the exchange component of the effective NN - interaction, $\rho^{(i)}(r,r')$ is the density matrix of colliding nuclei, $s=\left|\vec{r}_2-\vec{r}_1+\vec{R}\right|$ is the distance between interaction nucleons, M is reduced mass, $k(R)$ - local momentum of relative motion.

M3Y-Reid interaction is given in terms of Yukawa potential as follows [24]:

$$v_D(s)=7999.0\frac{e^{-4s}}{4s}-2134.25\frac{e^{-2.5s}}{2.5s}$$
$$v_{EX}(s)=4631.4\frac{e^{-4s}}{4s}-1787.87\frac{e^{-2.5s}}{2.5s}-7.8474\frac{e^{-0.7072s}}{-0.7072s}, \quad (6)$$

The equation of state of the optical potential is constructed depending on the density:

$$v_{D(EX)}(\rho,s)=f(\rho)v_{D(EX)}(s), \quad (7)$$

where ρ - is the density of the medium in which the nucleons is located. $f(\rho)$ - density dependence factor.

Density dependence factor takes the following form:

$$f(\rho)=C(1+\alpha\exp(-\beta\rho)-\gamma\rho), \quad (8)$$

C, α, β, γ -parameters of factor which reproduce the saturation process of nuclear matter in the calculations. The values are given in the Table 1.

The modified harmonic oscillator (MHO) model was used to calculate the matter density distribution of nuclei ^{13}C, ^{15}N [25]:

$$\rho(r)=\rho_0(1+\alpha(r/a)^2\exp(-(r/a)^2), \quad (9)$$

where a =1.81 fm and α =1.25 fm for ^{15}N and a =1.635 fm and α =1.403 fm for ^{13}C respectively.

The nucleon density distribution in the ^{19}F nucleus is expressed as a two-parameter Fermi [25] function as follows:

$$\rho(r)=\rho_0/(1+\exp(r-c)/z), \quad (10)$$

where c =2.59 fm and z =0.564 fm for ^{19}F.

Experimental data for the ^{15}N+ ^{13}C system are analyzed at energies E_{lab}=30.0, 32.0, and 45 MeV, and for ^{15}N+ ^{19}F are analyzed at energies E_{lab}=23.0, 26.0 and 29.0 MeV in the framework of OM, DF. The density dependent parameters included in the folding potentials are shown in Table 1.

Table 1. M3Y-Reid potentials coefficients

Density dependence	C	A	β(fm^3)	γ(fm^3)	K (MeV)
CDM3Y1-Reid	0.3429	3.0232	3.5512	0.5	188

In the framework of the optical model of DF, the real part of the optical potential is created by folding the NN interaction with the nuclear matter density distribution in the ground state of projectile nuclei $\rho^{(1)}(r_1)$ and target nuclei $\rho^{(2)}(r_2)$. Total interaction potential has DF potential is for the real part and WS volume potential is for the imaginary part:

$$U(r)=N_r\left[V^D(r)+V^{EX}(r)\right]-iW_0\left[1+\exp\left(\frac{r-R_W}{a_W}\right)\right]^{-1}+V_c(r), \quad (11)$$

where N_r - is the renormalization factor of the real potential part.

The obtained optimal potential parameters for ^{15}N+ ^{13}C and ^{15}N+ ^{19}F elastic scattering, together with the values of χ^2/N are presented in Table 2.

Table 2. Identified parameters as a result of the analysis of OM and DF for the ^{15}N+ ^{13}C and ^{15}N+ ^{19}F systems. Coulomb radius fixed: r_c=1.25fm

E MeV	Model	V_0 MeV	rv fm	av fm	W_0 MeV	r_W fm	a_W fm	`χ^2/N up to 90°	χ^2/N up to 180°	N_r
	^{15}N+ ^{13}C									
30.0	OM	133.09	1.09	0.54	9.92	1.18	0.49	6.5±0.01	23.93±0.8	-
	DFOM	CDM3Y1- Reid			9.79	1.24	0.49	7.74±0.01	29.62±0.5	0.92
32.0	OM	130	0.8	0.63	14.36	0.8	0.31	3.7±0.01	32.0±0.4	-
	DFOM	CDM3Y1- Reid			14.3	1.2	0.59	5.25±0.01	43.0±1.2	0.90
45.0	OM	124. 78	1.02	0.704	21.12	1.13	0.2	17.76±0.6	27.81±0.8	-
	DFOM	CDM3Y1- Reid			21.12	1.13	0.2	20.74±0.8	34.11±0.6	1.21
	^{15}N+ ^{19}F									
23.0	OM	83.55	1.19	0.53	33.53	1.34	0.29	0.17±0.01	1.94±0.08	-
	DFOM	CDM3Y1- Reid			33.64	1.4	0.39	1.05±0.01	2.02±0.01	0.817
26.0	OM	79.95	1.09	0.59	34.35	1.2	0.39	0.81±0.03	8.39±0.1	-
	DFOM	CDM3Y1- Reid			33.64	1.4	0.39	1.06±0.01	2.02±0.1	0.804
29.0	OM	78.93	1.16	0.57	36.0	1.31	0.28	1.65±0.01	5.52±0.08	-
	DFOM	CDM3Y1- Reid			36.64	1.37	0.39	1.69±0.02	6.3±0.2	0.812

Figures 1 and 2 depict the phenomenological and semi-microscopic cross sections (respectively) derived from the parameters of the ^{15}N+ ^{13}C system at E_{lab} =30.0, 32.0, 45.0 MeV, as well as the ^{15}N+ ^{19}F system at incident energies E_{lab} =23.0, 26.0, 29.0 MeV. Despite obtaining optimal parameters in the framework of OM and DF which will describe the experimental data in the forward angles, the description in the full angular range is difficult (it shows χ^2/N up to 180°).

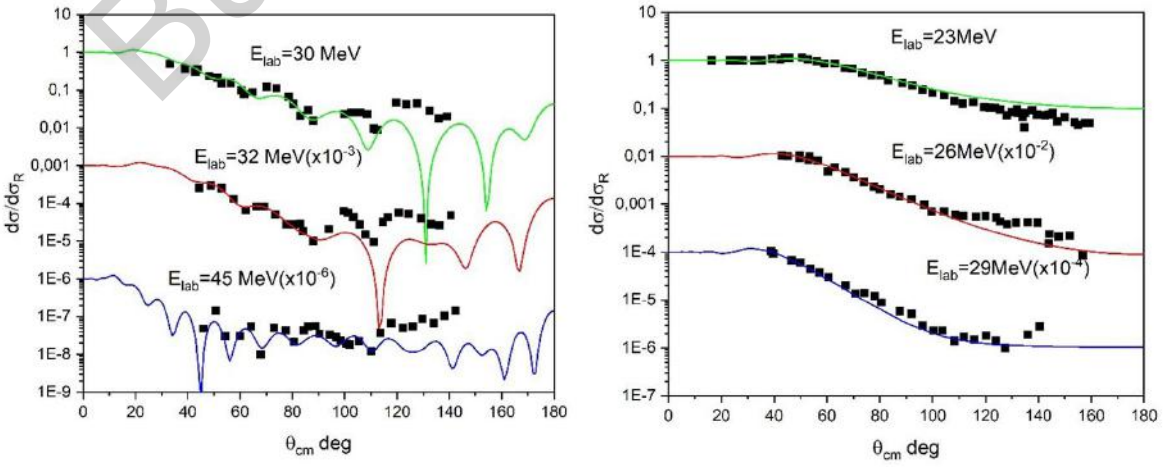

Fig.1. OM cross-sections for ^{15}N+ ^{13}C (left) and ^{15}N+ ^{19}F (right) nuclear systems

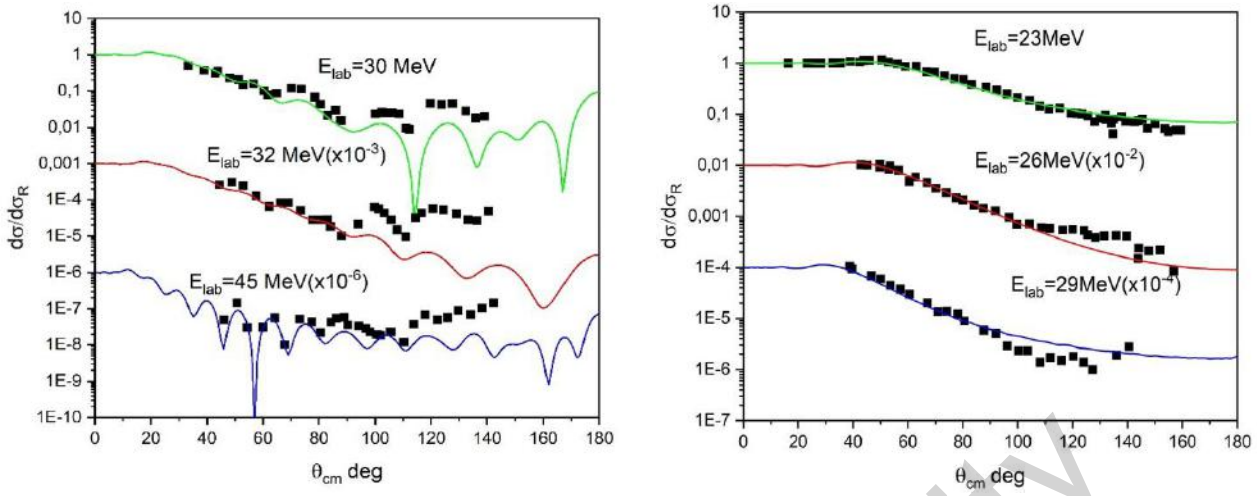

Fig.2. DF cross-sections for ^{15}N+ ^{13}C (left) and ^{15}N+ ^{19}F (right) nuclear systems

3. CRC analysis of ^{15}N +^{13}C, ^{15}N+ ^{19}F

The figures 3,4 demonstrate a significant increase in differential cross sections at backward angles, likely attributed to particle transfer processes. Such phenomena, involving the transfer of protons, deuterons, or alpha particles, have been extensively studied in previous works [26–29].

To accurately describe experimental data over the full angular range, the Coupled Reaction Channel (CRC) method is commonly employed. This approach extends the coupled channel framework to include nuclear rearrangement or transfer reactions, where one or more nucleons or composite particles (α, d particles) are transferred between the projectile and target nuclei. In this scenario, a composite projectile nucleus A=(a+x) interacts with a target nucleus b, transferring the particle x to form the final system B=(b+x). The nuclei a and b are referred to as cores. To compute the necessary wave functions, two critical parameters are needed: the number of nodes (N) in the radial wave function and the spectroscopic amplitudes (SA), which describe the decomposition of A and B into their constituent components a+x and b+x, respectively.

The Talmi-Moshinski transformation [30, 31] was employed to determine the quantum numbers of the cluster state, using the following formula:

$$2(N-1)+L=\sum_{i=1}^{n}2(n_i-1)+l_i, \qquad (12)$$

where N is the number of nodes of the radial wave function of relative motion (taking into account the node at $r=0$) and L is the corresponding orbital momentum of the cluster, n_i, l_i are quantum numbers of components of a cluster of nucleons in harmonic oscillator model, Σ denotes the sums of similar quantities for nucleons entering a cluster in a bound state.

The differential cross section is the square of the sum of amplitudes from the pure elastic scattering and the exchange mechanism of the cluster transfer, as follows [8]:

$$\frac{d\sigma}{d\Omega}=\left|f_{el}(\theta)+e^{i\alpha}Sf_{tr}(\pi-\theta)\right|^2, \qquad (13)$$

here $f_{el}(\theta)$ is the elastic scattering amplitude, f_{tr} is the transfer amplitude calculated using the distorted wave method with the replacement $\theta=\pi-\theta$, S is the product of the two spectroscopic amplitudes (SA), parameter $\alpha=pi$ (coherence of amplitudes).

Experimental data for the ^{15}N+ ^{13}C system are analyzed at energies E_{lab} =30.0, 32.0, 45 MeV and for ^{15}N+ ^{19}F are analyzed at energies E_{lab} =23.0, 26.0, 29.0 MeV in the framework of CRC. The cluster quantum numbers for the overlap used in CRC calculations are listed in Table 3.

Table 3. Cluster quantum number for the overlaps for the $^{15}N+ ^{13}C$ and $^{15}N+ ^{19}F$ systems used in our calculations.

Overlap	N	L	S	J=L+S	Binding Energy (MeV)
$<^{13}C+d\|^{13}C>$	3	2	1	1	16.16
$<^{15}N+\alpha\|^{15}N>$	2	1	0	1	4.01

The OM potentials presented in Table 2 were also used in the study of the elastic transfer of d for the $^{15}N+ ^{13}C$ system and α cluster transfer in the $^{15}N+ ^{19}F$ scattering. These calculations were performed using only one adjustable parameter SA (for the $^{15}N \rightarrow ^{13}C$ + d -configuration and $^{19}F \rightarrow ^{15}N$ + α-configuration). Parameter SA is shown in Table 4 for each nuclear system.

Table 4. Data of SA parameters for each nuclear system.

E_{lab} MeV	SA	χ^2/N up to 180°
$^{15}N+ ^{13}C$		
30	0.35±0.001	7.95±0.01
32	0.3±0.006	16.05±0.001
45	0.35±0.004	20.8±0.2
$^{15}N+ ^{19}F$		
23	0.3±0.008	1.85±0.01
26	0.3±0.006	7.84±0.3
29	0.3±0.004	4.45±0.2

The extracted average SA values for $^{15}N \rightarrow ^{13}C$ + d, $^{19}F \rightarrow ^{15}N$ + α -configuration are 0.33 and 0.3. As shown in Figure 3 the agreement between the experimental data at large angles and the CRC calculations, which took into account the mechanism of the transfer of the d - cluster transfer in the $^{13}C(^{15}N, ^{13}C)^{15}N$ reaction and α - cluster transfer in the ^{19}F (^{15}N, ^{19}F) ^{15}N reaction is quite good.

The values of SA we derived for the above systems are in good agreement with the data from the publications of Rudchik et al [31] and [13]. In the present work, the energy dependencies are found for the real and imaginary parts of the potential (figure 4). For the potential set, energy dependencies are described by the linear functions V = 147.09–0.499E and W = −8.59 + 0.66E for $^{15}N+ ^{13}C$ and V = 88.85–0.22E and W = 22.92 + 0.41E for the $^{15}N+ ^{19}F$ scattering system.

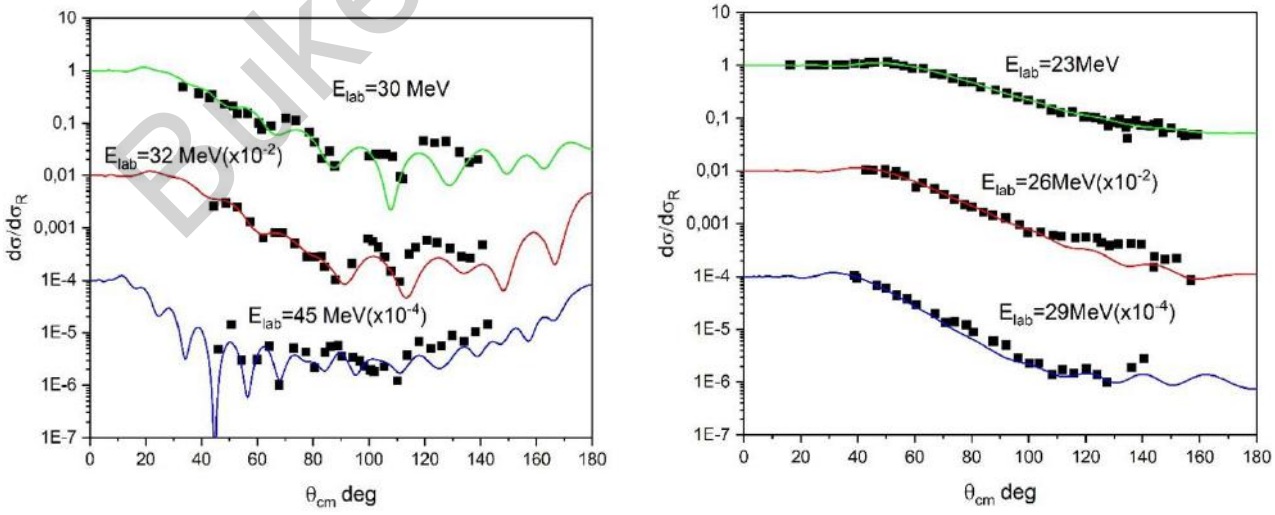

Fig.3. CRC cross-sections for $^{15}N + ^{13}C$ (left) and $^{15}N + ^{19}F$ (right)

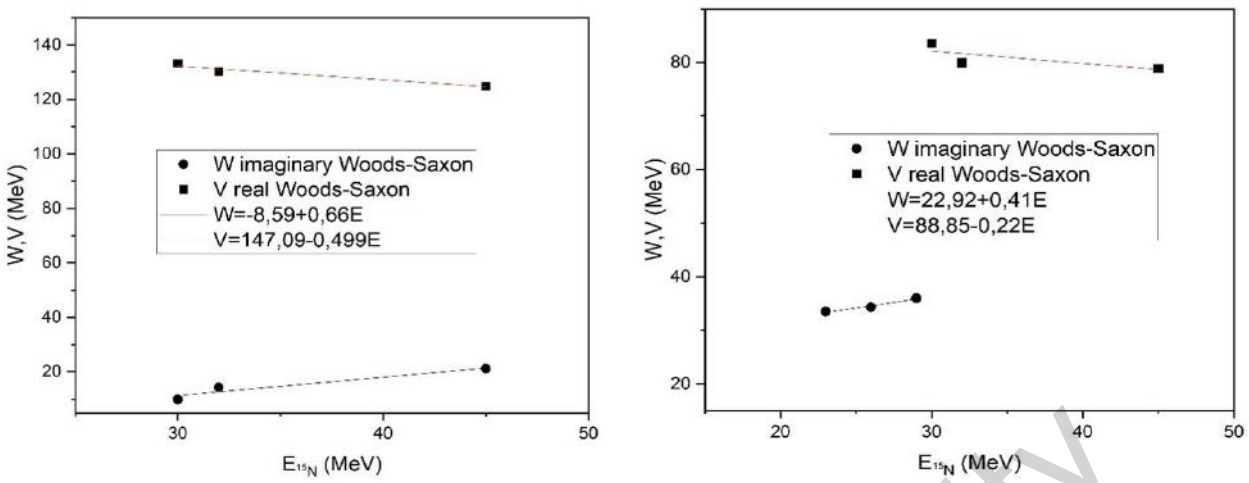

Fig.4. Energy dependence of $^{15}N + ^{13}C$ (left) and $^{15}N + ^{19}F$ (right)

4. Conclusion

New information on the parameters of optical potentials and reaction cross sections was obtained from the analysis of experimental data on the angular distributions of elastic scattering for the $^{15}N + ^{19}F$ and $^{15}N + ^{13}C$ systems. The energy dependences of the real and imaginary components of the nuclear potential depth were determined. A more physically meaningful set of optical potential parameters was also obtained by employing the DF model and the CRC.

Within the semi-microscopic framework, a folding potential based on the CDM3Y1-Reid interaction was constructed using the double-folding (DF) model. The phenomenological analysis revealed relative errors ranging from 0.17 to 1.6 for $^{15}N + ^{19}F$ and from 3.7 to 17.6 for $^{15}N + ^{13}C$ when comparing experimental and theoretical cross-sections. In the semi-microscopic analysis, the renormalization coefficients (Nr) of the microscopic potentials were determined to be 0.8–0.817 for $^{15}N + ^{19}F$ and 0.92–1.21 for $^{15}N + ^{13}C$. To fully describe the experimental data across the entire angular range, calculations were conducted using the Coupled Reaction Channel (CRC) method implemented in the FRESCO program. This approach incorporated elastic scattering, modeled using the optical model (OM), and the exchange mechanism, which accounted for cluster transfer—an α-cluster for $^{15}N + ^{19}F$ and a d-cluster for $^{15}N + ^{13}C$ — calculated with the distorted wave method.

As a result of this analysis, spectroscopic amplitude (SA) values were determined for the configurations $^{19}F \rightarrow ^{15}N + \alpha$ (average SA=0.3) and $^{15}N \rightarrow ^{13}C + d$ (average SA=0.33). These SA values show strong consistency with data reported by other researchers, underscoring the reliability of the findings.

Conflict of interest statement

The authors declare that they have no conflict of interest in relation to this research, whether financial, personal, authorship or otherwise, that could affect the research and its results presented in this paper.

CRediT author statement

Akhat R. - conceptualization, methodology, investigation; **Amangeldi N.** - supervision, project administration; **Baratova A.**- writing-original draft, writing-review, editing; **Anuar A. -** vizualization; **Raiymbekov Ye.** - software, investigation; **Yergaliuly G.** - conceptualization, formal analysis.

Acknowledgements

This work was carried out by the Science Committee of the Ministry of Science and Higher Education of the Republic of Kazakhstan (Grant No. AP19680284).

References

1 Soldatkhan D., Amangeldi N., Baltabekov A.S., Yergaliuly G., Mauyey B. (2022).= Investigation of the energy dependence of the interaction potentials of the $^{16}O+^{12}C$ nuclear system with a semi-microscopic method. *Eurasian Physical Technical Journal*, *19, 3(41),* 39-44, https://doi.org/10.31489/2022No3/39-44

2 Amar A., Hamada A., Burtebayev N., Amangeldy N. (2011) Study of scattering ^{1}H, ^{12}C and ^{16}O nuclei on 1P-shell at energy near the Coulomb barrier. *Int. J. Mod. Phys. E*, *20*, 980–986, https://doi.org/10.1142/S0218301311019106

3 Wang K., Yang Y.Y., Guimarães V., Pang D.Y., Duan F.F., Sun Z.Y. (2023) Elastic scattering investigation of radioactive ^{13}B and ^{13}O projectiles on a ^{208}Pb target at intermediate energies. *Phys. Rev. C*, *105*, 054616, https://doi.org/10.1103/PhysRevC.105.054616

4 Yang G., Duan F.F., Wang K., Yang Y.Y., Sun Z.Y., Guimarães V., Pang D.Y., Chen W.D., Jin L., Xu S.W., Ma J.B., Ma P., Bai Z., Wang L.H., Liu Q., Ong H.J., Lv B.F., Guo S., Raju M.K., Wang X.H., Li R.H., Zhang Y.H., Zhou X.H., Hu Z.G., Xu H.S. (2023) Elastic scattering of ^{13}C and ^{14}C isotopes on a ^{208}Pb target at energies around five times the Coulomb barriers. *Chin. Phys. C*, *3*, 034001, https://doi.org/10.1088/1674-1137/ad1678

5 Kundalia K., Gupta D., Ali S.M., Saha S.K., Tengblad O., Ovejas J.D., Perea A., Martel I., Cederkall J., Park J., Szwec S., Moro A.M. (2022) Study of elastic and inelastic scattering of ^{7}Be + ^{12}C at 35 MeV. *Phys. Lett. B*, *833*, 137294, https://doi.org/10.1016/j.physletb.2022.137294

6 La Fauci L., Spatafora A., Cappuzzello F., Agodi C., Carbone D., Cavallaro M., Lubian J., Acosta L., Amador-Valenzuela P. (2021) ^{18}O +^{76}Se elastic and inelastic scattering at 275 MeV. *Phys. Rev. C*, *104*, 054610, https://doi.org/10.1103/PhysRevC.104.054610

7 Nassurlla M., Burtebayev N., Karakozov B.K., Sakuta S.B., Boztosun I., Amangeldi N., Morzabayev A.K., Yergaliuly G., Alimov D.K., Burtebayeva J., Nassurlla M., Mauyey B., Kucuk Y., Hamada S., Sabidolda A., Khojayev R. (2021) New measurements and analysis of elastic scattering of ^{13}C by ^{9}Be nuclei in a wide energy range. *Eur. Phys. J. A*, *57*, 1–9, https://doi.org/10.1140/epja/s10050-021-00539-z

8 Hamada S., Burtebayev N., Gridnev K.A., Amangeldi N. (2011) Analysis of alpha-cluster transfer in $^{16}O+^{12}C$ and $^{12}C+^{16}O$ at energies near Coulomb barrier. *Nucl. Phys. A*, *859*, 29–38, https://doi.org/10.1016/j.nuclphysa.2011.04.006

9 Burtebayev N., Nassurlla M., Sabidolda A., Sakuta S.B., Karakhodzhaev A.A., Ergashev F., Rusek K., Piasecki E., Trzcinska A., Wolińska-Cichocka M., Mauyey B., Janseitov D., Zalewski B., Hamada S., Kemper K.W., Ibraheem A.A. (2019) Measurement and analysis of ^{10}B +^{12}C elastic scattering at energy of 41.3 MeV. *Int. J. Mod. Phys. E*, *28*, 1950028, https://doi.org/10.1142/S0218301319500289

10 Phuc N.T.T., Phuc N.H., Khoa D.T. (2018) Direct and indirect α transfer in elastic ^{16}O + ^{12}C scattering. *Phys. Rev. C*, *98*, 1–13, https://doi.org/10.1103/PhysRevC.98.024613

11 Gamp A., Braun-Munzinger P., Gelbke C.K., Harney H.L., Bohlen H.O., Bohn W., Hildenbrand K.D., Kuzminski J., von Oertzen W., Tserruya I. (1975) Interfering proton and neutron transfer in the reaction ^{13}C (^{15}N, ^{14}N)^{14}C. *Nucl. Phys. A*, *250*, 341–350, https://doi.org/10.1016/0375-9474(75)90264-X

12 Gamp A., von Oertzen W., Bohlen H.G., Feil M., Walter R.L., Marquardt N. (1973) Elastic Scattering of ^{15}N on ^{19}F, ^{19}F on ^{18}O and ^{19}F on ^{16}O at low energies and elastic transfer. *Z. Phys. A*, *304*, 283–304, https://doi.org/10.1007/BF01399327

13 Nassurlla M., Burtebayev N., Sakuta S.B., Karakozov B. K., Nassurlla M., Burtebayeva J., Khojayev R., Sabidolda A., Yergaliuly G. (2022) Deuteron scattering and (d, t) reaction on ^{11}B at an energy of 14.5 MeV. *Nuclear Physics A*, *1023*, 122448. https://doi.org/10.1016/j.nuclphysa.2022.122448

14 Ibraheem A.A., Al-Amri H. (2022) Analysis of $^{4,6,8}He+^{208}Pb$ elastic scattering at E = 22 MeV using various potentials. *Rev. Mex. Fis.*, *58*, 4–10, https://doi.org/10.31349/revmexfis.68.051201

15 Khoa D.T., von Oertzen W., Bohlen H.G. (1994) Double-folding model for heavy-ion optical potential: Revised and applied to study ^{12}C and ^{16}O elastic scattering. *Phys. Rev. C*, *49*, 1652–1668, https://doi.org/10.1103/PhysRevC.49.1652

16 Alsaif N.A.M., Hamada S., Farid M.E.A., Alotaibi B.M., Alotiby M., Mohammed A., Awad A. (2023) Elastic scattering of $^{7}Li+^{58}Ni$: a phenomenological and microscopic analysis. *Rev. Mex. Fis.*, *69*, 1–11, https://doi.org/10.31349/revmexfis.69.021201

17 Thompson I.J. (1988) Coupled reaction channels calculations in nuclear physics. *Comput. Phys. Rep.*, *7*, 167–212, https://doi.org/10.1016/0167-7977(88)90005-6

18 Boztosun I., Dagdemir Y., Bayrak O. (2005) The examination of the $^{12}C+$ ^{24}Mg elastic scattering around the Coulomb barrier. *Physics of Atomic Nuclei, 68*, 1153-1159. https://doi.org/10.1134/1.1992570

19 Khoa D.T., Satchler G.R. (2000) Generalized folding model for elastic and inelastic nucleus–nucleus scattering using realistic density dependent nucleon–nucleon interaction. *Nucl. Phys. A*, *668*, 3–41, https://doi.org/10.1016/S0375-9474(99)00680-6

20 Khoa D.T., Satchler G.R., von Oertzen W. (1997) Nuclear incompressibility and density dependent NN interactions in the folding model for nucleus-nucleus potentials. *Physical Review C, 56*, 954–969, https://doi.org/10.1103/PhysRevC.56.954

21 Khoa D.T., von Oertzen W. (1995) Refractive alpha-nucleus scattering: a probe for the incompressibility of cold nuclear matter. *Phys. Lett. B*, *342*, 6–12, https://doi.org/10.1016/0370-2693(94)01393-Q

22 Khoa D.T. (2001) α-nucleus optical potential in the double-folding model. *Physical Review C*, 63, 034007. https://doi.org/10.1103/PhysRevC.63.034007

23 Soldatkhan D., Yergaliuly G., Amangeldi N., Mauyey B., Odsuren M., Ibraheem A. A., Hamada S. (2022) New Measurements and Theoretical Analysis for the ^{16}O+ ^{12}C Nuclear System. *Brazilian Journal of Physics*, *52,* 152. https://doi.org/10.1007/s13538-022-01153-0

24 De Vries H., De Jager C.W., De Vries C. (1987) Nuclear Charge-Density-Distribution Parameters From Elastic Electron Scattering. *At. Data Nucl. Data Tables*, *36*, 495–536, https://doi.org/10.1016/0092-640X(87)90013-1

25 Amangeldi N., Burtebayev N., Sakuta S.B., Nassurlla M., Burtebayeva J., Nassurlla M., Yergaliuly G., Sabidolda A., Rusek K., Trzcinska A., Wolińska-Cichocka M., Mauyey B. (2020) Study of elastic scattering of 10B ions on ^{12}C nuclei at the energy of 17.5 MeV. *Acta Phys. Pol. B*, *51*, https://doi.org/10.5506/APhysPolB.51.757

26 Takai H., Koide K., Bairrio Nuevo A., Dietzsch O. (1988) α-transfer contribution to ^{10}B+^{14}N elastic scattering. *Phys. Rev. C*, *38*, 741–747, https://doi.org/10.1103/PhysRevC.38.741

27 Rudchik A.T., Budzanowski A., Chernievsky V.K., Czech B., Głowacka L., Kliczewski S., Mokhnach A.V., Momotyuk O.A., Omelchuk S.E., Pirnak Val.M., Rusek K., Siudak R., Skwirczyńska I., Szczurek A., Zemło L. (2001) The ^{11}B+^{12}C elastic and inelastic scattering at Elab(^{11}B) = 49 MeV and energy dependence of the ^{11}B+^{12}C interaction. *Nucl. Phys. A*, *695*, 51–68, https://doi.org/10.1016/S0375-9474(01)01106-X

28 Gridnev K.A., Mal'tsev N.A., Burtebaev N., Amangel'dy N., Hamada S. (2012) Role of the inelastic transfer channel in elastic ^{16}O+ ^{12}C scattering over a wide range of energies. *Bulletin of the Russian Academy of Sciences: Physics*, *76*, 934-937. https://doi.org/10.3103/S106287381208014X

29 Burtebayev N., Sadykov T.K., Boztosun I., Amangeldi N., Alimov D., Kerimkulov Z., Burtebayeva J., Maulen Nassurlla, Kurakhmedov A., Sakuta S.B., Karakoc M., Ibraheem Awad A., Kemper K.W., Hamada Sh. (2020). New measurements and reanalysis of ^{14}N elastic scattering on ^{10}B target. *Chinese Physics C, 44*, 115-123. https://doi.org/10.1088/1674-1137/abab89

30 Keeley N., Alamanos N., Kemper K.W., Rusek K. (2009) Elastic scattering and reactions of light exotic beams. *Prog. Part. Nucl. Phys.*, *63*, 396–447, https://doi.org/10.1016/j.ppnp.2009.05.003

31 Rudchik A.T., Rudchik A.A., Kutsyk O.E., Kemper K.W., Rusek K., Piasecki E., Trzcińska A., Kliczewski S., Koshchy E.I., Pirnak Val.M., Ponkratenko O.A., Strojek I., Plujko V.A., Sakuta S.B., Siudak R., Ilyin A.P., Stepanenko Yu.M., Shyrma Yu.O., Uleshchenko V.V. (2019) ^{12}C(^{15}N, ^{14}C)^{13}N reaction at 81 MeV. Competition between one and two particle transfers. *Nucl. Phys. A*, *992*, 121638, https://doi.org/10.1016/j.nuclphysa.2019.121638

AUTHORS' INFORMATION

Raimbek, Akhat – PhD student, Eurasian National University, National Laboratory Astana, Astana, Kazakhstan; Scopus Author ID: 57226571776; https://orcid.org/0000-0002-7634-0525; akhat.raimbek22@gmail.com

Amangeldi, Nurlan – PhD, Assistant Professor, Department of Nuclear Physics, New Materials and Technologies, L.N. Gumilyov Eurasian National University, Astana, Kazakhstan; Scopus Author ID: 37065699200; https://orcid.org/0000-0002-9416-5425 ; Nur19792@mail.ru

Baratova, Aliya – Candidate of physical and mathematical sciences, Senior Lecturer, Department of Nuclear Physics, New Materials and Technologies, L.N. Gumilyov Eurasian National University, Astana, Kazakhstan; Scopus Author ID: 55221822500; https://orcid.org/0000-0002-7015-3657 , baratova_aa@enu.kz

Anuar, Aida – PhD student, Eurasian National University, Astana, Kazakhstan, https://orcid.org/0009-0006-8587-8673 ; Aeedaassylbekova6@gmail.com

Raiymbekov, Ye. – PhD student, Eurasian National University , National Laboratory Astana, Astana, Kazakhstan, Scopus Author ID: 58532271000; https://orcid.org/0000-0003-3380-9263; esimray@mail.ru

Yergaliuly, Gani – PhD, National Laboratory Astana, Kazakhstan, Scopus Author ID: 57216951648; https://orcid.org/0000-0002-7443-8561; yergaliuly.gani@gmail.com